Journal of Physics: Conference Series **2462** (2023) 012047 doi:10.1088/1742-6596/2462/1/012047

Low energy muon study of the p-n interface in chalcopyrite solar cells

H V Alberto*[1], R C Vilão[1], E F M Ribeiro[1], J M Gil[1], M A Curado[1,2], J P Teixeira[2,3,4], P A Fernandes[2,3,4], J M V Cunha[2,3,5], P M P Salomé[2,5], M Edoff[6], M I Martins[7,8], T Prokscha[8], Z Salman[8], and A Weidinger[9]

[1] CFisUC,Department of Physics, University of Coimbra, R. Larga, Coimbra P-3004-516, Portugal
[2] International Iberian Nanotechnology Laboratory, 4715-330 Braga, Portugal
[3] i3N,Departamento de Física da Universidade de Aveiro, Campus Universitário de Santiago, 3810-193 Aveiro, Portugal
[4] CIETI, Departamento de Física, Inst. Sup. de Eng. do Porto, Inst. Pol. do Porto, Porto 4200-072, Portugal
[5] Departamento de Física da Universidade de Aveiro, Campus Universitário de Santiago, 3810-193 Aveiro, Portugal
[6] Ångström Laboratory, Solid State Electronics, Ångström Solar Center, Uppsala University, SE-75121 Uppsala, Sweden
[7]Advanced Power Semiconductor Laboratory, ETH Zürich, Switzerland, 8092 Zürich, Switzerland
[8]Laboratory for Muon Spin Spectroscopy, Paul Scherrer Institut, CH-5232 Villigen PSI, Switzerland
[9]Department ASPIN, Helmholtz-Zentrum Berlin für Materialien und Energie, 14109 Berlin, Germany

E-mail: `lena@uc.pt`

Abstract. The slow muon technique was used to study the p-n junction of chalcopyrite solar cells. A defect layer near the interface was identified and the passivation of the defects by buffer layers was studied. Several cover layers on top of the chalcopyrite Cu(In,Ga)Se_2 (CIGS) semiconductor absorber were investigated in this work, namely CdS, ZnSnO, Al_2O_3 and SiO_2. Quantitative results were obtained: The defect layer extends about 50 nm into the CIGS absorber, the relevant disturbance is strain in the lattice, and CdS provides the best passivation, oxides have a minor effect. In the present contribution, specific aspects of the low-energy muon technique in connection with this research are discussed.

1. Introduction

Solar cells based on chalcopyrite absorbers are a promising alternative or complement to Si solar cells [1, 2]. Cu(In,Ga)Se_2 (CIGS) is a promising absorber material for thin film solar cells [3, 4]. It is under intense investigation in academic and industrial laboratories [1, 3]. However, further improvements in efficiency and fabrication methods are needed for widespread industrial implementation. In research, a particular focus is on improving the interface at the transition from the p-type absorber to the n-type window layer. The matching of these two areas is achieved by introducing buffer layers.

Low-energy muon spectroscopy is practically the only way to obtain depth-resolved information about the interfacial region at the nanometer scale [5, 6]. Our main results were published in Advanced Materials Interfaces [7]. We present here a brief summary of this work with special focus to the µSR aspects of the data.

2. Experimental details

The samples for this research were obtained from the Ångström laboratory in Uppsala Sweden ([8, 9, 10]). Their standard solar cells reach efficiencies of up to 18.6 %. For the present μSR experiment, the solar cells were processed only up to the buffer layer so that the slow muons could reach the interface. Different buffer layers were used, namely CdS, ZnSnO, Al_2O_3, SiO_2. For Al_2O_3 two samples were prepared with two different widths (4 and 22 nm). For SiO_2, two samples were investigated, one with a positive, and the other with a negative interface charge, named as SiO_2^+ and SiO_2^-, respectively [11]. The muon spin spectroscopy (μSR) measurements were performed at the low energy muons (LEM) instrument [12] of the Swiss Muon Source, Paul Scherrer Institut, Switzerland. Positive muons were implanted in the samples at an external magnetic field, $B = 10$ mT, in a transverse field (TF) geometry and at a temperature $T = 50$ K. Depth profiles are obtained by varying the muon implantation energy in the range $3 - 25$ keV.

3. Results

A typical µSR time spectrum of a CIGS thin film with a cover layer is a gaussian-damped oscillation at the Larmor frequency. Part of the µSR signal is missing, that is the total amplitude of the signal is smaller than the corresponding amplitude of a silver calibration. We use the normalized amplitude of this signal, i.e., the diamagnetic fraction, as a marker for depth profiling. This parameter is sensitive to structural perturbations, as will be discussed in more detail in the discussion section. The reason for the sensitivity is that structural perturbations reduce the formation of a bound muon configuration and thus causes a decrease in the fraction. Figure 1 shows the measured depth profile of the diamagnetic fraction for a CIGS sample covered with a 20 nm thick ZnSnO top layer.

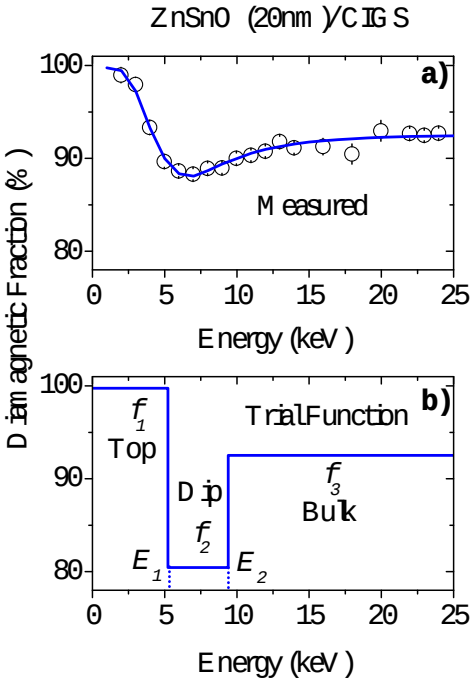

Figure 1. a) Measured diamagnetic fraction for the ZnSnO(20 nm)/CIGS sample as a function of the implantation energy. b) Trial function for the deconvolution procedure. The convolution of this distribution with the resolution function gives the solid line in the upper frame.

Three regions can be distinguished: A high fraction at low implantation energies, then a dip in the middle region and finally a leveling off of the fraction at higher implantation energies. We identify the first part of the profile with the fraction in the top layer and the part at the higher implantation energies with the fraction in bulk CIGS. There is apparently a dip in the fraction in the intermediate implantation range which corresponds to the interface region of the layer structure. In principle, one could also use another parameter of the signal for profiling, e.g. the relaxation [13, 14], but in the present case the diamagnetic component is the most sensitive parameter to perturbations in CIGS, which is the information of interest for solar cells, that we want to access. It should also be mentioned that due to the range distribution of the implanted muons, the signal generally contains two components, one from the top layer and one from CIGS, and that a two-component fit should be applied. However, since the relaxation, frequency, and phase are similar for both materials, the components cannot be separated. For profiling purposes, we assume that the fraction of the one-component fit is equal to the sum of the two individual fractions.

The measured profile is smeared out due to the finite resolution which is due to the range distribution of the implanted muons. In the present case, the half-width of the range distribution is in the order of 20 to 30 nm. To obtain more precise information about the fractions in the different areas, deconvolution with the resolution function is therefore necessary [13, 15, 7]. This is done in this work by assuming a trial function and fitting it, after convolution with the resolution function, to the measured profile. For a given muon implantation energy E, a resolution function, $P(x, E)$, representing the probability that a muon stops at a given film depth, x, can be obtained from Monte Carlo Simulations using TRIM.SP code [16, 17]. However, as shown in [7] it is more convenient to perform the deconvolution in the energy space, using an adequate variable change from x to E'. The conversion between the resolution function $P(x, E)$ and $P(E', E)$ is explained in ref [7] and discussed in detail in [18] . Therefore, the measured diamagnetic fraction $f_{\mathrm{dia}}^{\mathrm{exp.}}(E)$ is related with the real distribution by

$$f_{\mathrm{dia}}^{\mathrm{exp.}}(E) = \int_0^\infty P(E', E)\, f_{\mathrm{dia}}(E')\, dE' \tag{1}$$

The trial function is parametrised as shown in Fig. 1b. It contains five adjustable parameters: the three fractions f_1, f_2 and f_3 of the top, dip and bulk region, respectively, and the two energies E_1 and E_2 at the transition from the top layer to CIGS and the transition from the dip to bulk, respectively. The fit result is shown as solid line in Fig. 1a. The same procedure was used for the other samples. Three representative examples are shown in Fig.2.

In case of the bare CIGS sample (Fig.2,a)), a large dip is observed, indicating a strong perturbation of the lattice in the near-surface region of CIGS. This strong disturbance extends about 50 nm into the sample; the relative change of the fraction is about 11.4 %. For the other two samples, the dip is smaller, but it is not clear whether the width or the depth of the dip is reduced since a large correlation exists between these two parameters in the fitting. We therefore evaluated only the product of these two quantities and call it the dip size.

Figure 3 gives an overview of the passivation effect of the different cover layers. We define the passivation effect as the ratio between the dip size of the bare CIGS sample and the dip size of the sample with a top layer. The value 1.00 means that the dip size is not reduced by the cover layer, i.e. no passivation occurs; the larger this ratio, the larger the passivation effect. It can be seen that CdS yields the best passivation, the oxide layer have a much weaker effect on restoring the crystal ordering.

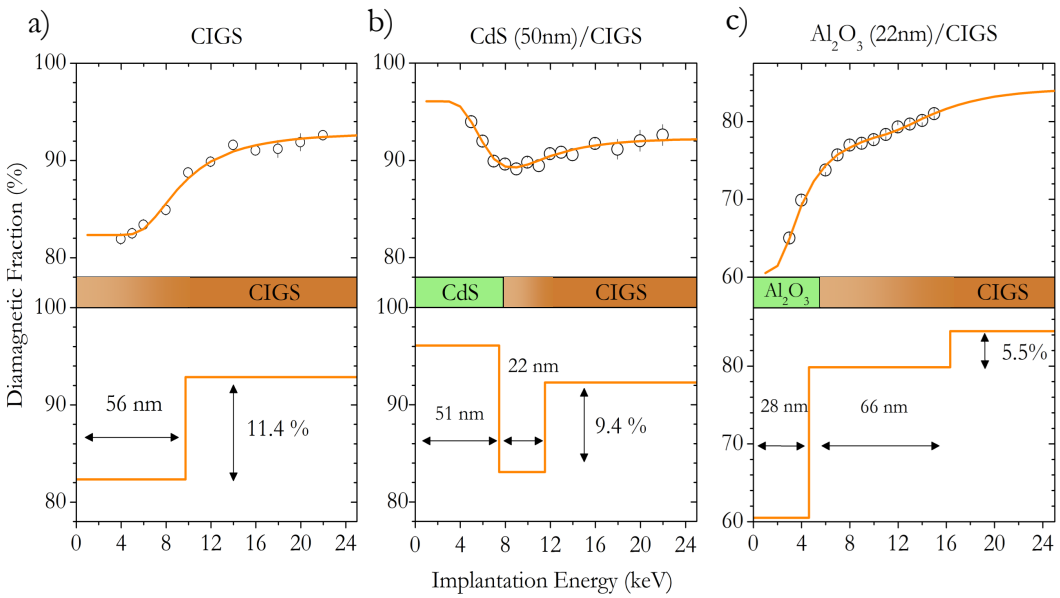

Figure 2. Depth profiles (diamagnetic fraction versus implantation energy) for the samples indicated at the top of each frame. The upper part of each frame shows the measured diamagnetic fraction along with the fitting curve. The lower part displays the depth distribution after deconvolution. The indicated layer thicknesses are obtained by converting the implantation energy in average range. The change of the fraction in the dip relative to the bulk value is indicated: $\Delta f/f \cdot 100$ %. Data from [7].

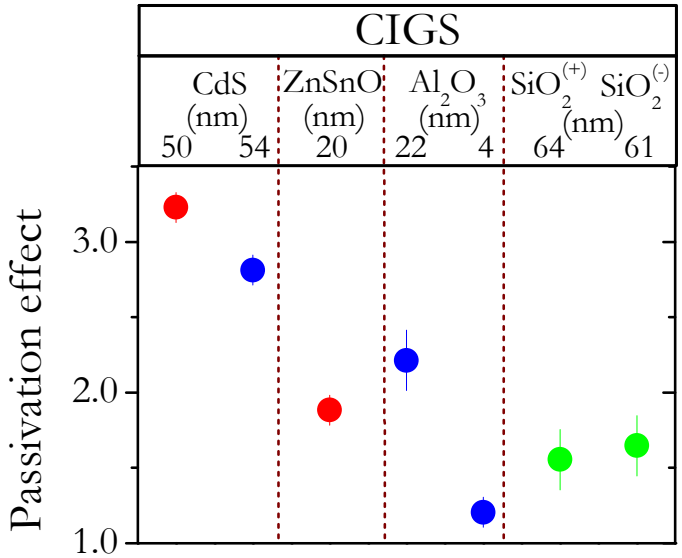

Figure 3. Passivation effect of the cover layers which are indicated on top of the figure (the chemical symbols and the thickness in nm are given). We define the passivation effect as the ratio between the dip size of the uncovered and the dip size of the covered CIGS sample. Different colors indicate different measurement runs and sample batches. Data from [7].

4. Discussion and Conclusion

Why is the diamagnetic fraction sensitive to disorder in the lattice? We suggest that the formation of the diamagnetic configuration, which requires rearrangement of the lattice around the muon, occurs more easily in an ordered lattice than in a distorted lattice. Structural defects such as vacancies and interstitials lead to a long-range perturbation of the lattice (Fig. 4), which affects the formation of the diamagnetic fraction. The reaction of the muon with the lattice can be considered as a jump over a potential barrier [19, 20, 21, 22]. Since the height of this barrier increases with disorder, the reaction probability decreases and a smaller fraction is obtained.

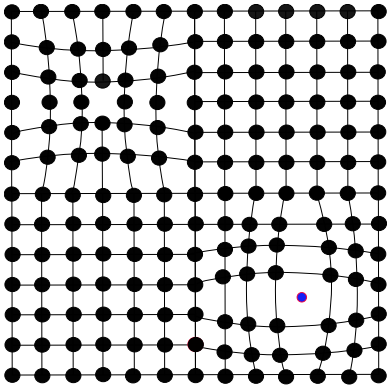

Figure 4. Defects (vacancy at left upper corner, interstitial at right lower corner) induce a long-range disturbance of the lattice which affects the formation probability of the diamagnetic signal.

In the present case, where the diamagnetic fraction is the dominant component, lattice disturbance *reduces* the diamagnetic fraction. In other cases, e.g. in Si, the diamagnetic fraction is small and the major reaction channel is towards interstitial muonium. In this case, an increase of the barrier for the dominant reaction reduces the interstitial muonium formation and causes an *increase* of the diamagnetic fraction.

The main physical result of the present experiment is that a near-interface defect layer has been identified which extends about 50 nm into the CIGS absorber. Buffer layers on top of CIGS can heal the defect-induced lattice disturbances: CdS provides the best healing effect, oxide layers are less effective. It is known in the literature that CdS gives the best efficiency [4]. However, because of the toxicity of Cd, other materials such as oxides are tried. Our experiment shows that the oxides are less effective in defect passivation than CdS. This is in accordance with the literature [10, 11]. The exact mechanism of defect passivation by CdS is not known. We suggest that particle diffusion from the buffer into CIGS plays a role for the healing of the disturbance.

On the methodological side, a new procedure for deconvolution of the depth profiles has been developed. The deconvolution of the measured profile in energy space is more direct and intuitively understandable and, above all, much simpler than deconvolution in real space. In the energy space, calculation of range distributions for each specific sample is not necessary since universal range distributions, once provided, can be used for any sample. In summary, using an adequate methodology, the use of slow muon technique provides a unique quantitative method to measure the spatial extent of the passivation effect of the different cover layers in chalcopyrite solar cells.

Acknowledgments

This work is based on experiments performed at the Swiss Muon Source (SμS), Paul Scherrer Institute, Villigen, Switzerland. A. W. thanks Prof. Klaus Lips for the invitation to the Helmholtz-Zentrum Berlin für Materialien und Energie. This work was supported with funds from FEDER (Programa Operacional Factores de Competitividade COMPETE) and by national

funds from FCT - Fundação para a Ciência e Tecnologia, I. P. (Portugal) under projects PTDC/FIS-MAC/29696/2017, PD/BD/142780/2018, UID/04564/2020, UID/04730/2020, UID/50025/2020.

References

[1] Kato T 2017, Cu(In,Ga)(Se,S)$_2$ Solar cell research in Solar Frontier: Progress and current status, *Jpn. J. Appl. Phys.* **56**, 04CA02.
[2] Nakamura M, Yamaguchi K, Kimoto Y, Yasaki Y, Kato T and Sugimoto H 2019, Cd-Free Cu(In,Ga)(Se,S)2 Thin-Film Solar Cell With Record Efficiency of 23.35%, *IEEE Journal of Photovoltaics*, 1863.
[3] D. Abou-Ras et al 2017, Innovation highway: Breakthrough milestones and key developments in chalcopyrite photovoltaics from a retrospective viewpoint, *Thin Solid Films 633* 2.
[4] T. Feurer et al 2017, Progress in thin film CIGS photovoltaics – Research and development, manufacturing, and application, *Prog. Photovolt: Res. Appl. 25* 645.
[5] Alberto H V et al 2018, Slow-muon study of quaternary solar-cell materials: single layers and p-n junctions, *Physical Review Materials* **2** 025402.
[6] Martins M I M, Kumar P, Woerle J, Ni X, Grossner U, Prokscha T, 2022, Defect profiling of oxide-semiconductor interfaces using low-energy muons, *Preprint* arXiv.2206.00925
[7] Alberto H V et al 2022, Characterization of the interfacial defect layer in chalcopyrite solar cells by depth-resolved muon spin spectroscopy,*Adv. Mater. Interfaces*, 2200374
[8] Lindahl J, Zimmermann U, Szaniawski P, Törndahl T, Hultqvist A, Salomé P M P, Platzer-Björkman C and Edoff M 2013, Inline Cu(In,Ga)Se$_2$ co-evaporation for high-efficiency solar cells and modules, *IEEE Journal of Photovoltaics* **3**, 1100.
[9] Lindahl J, Wätjen J T, Hultqvist A, Ericson T, Edoff M and Törndahl T 2013, The effect of $Zn_{1-x}Sn_xO_y$ buffer layer thickness in 18.0% efficient Cd-free Cu(In,Ga)Se$_2$ solar cells, *Progress in Photovoltaics: Research and Applications* **21**, 1588.
[10] Curado M A et al 2020, Front passivation of Cu(In,Ga)Se$_2$ solar cells using Al_2O_3 : culprits and benefits, *Applied Materials Today* **21**, 100867.
[11] Cunha J M V et al 2018, Insulator materials for interface passivation of Cu(In,Ga)Se$_2$ thin films, *IEEE Journal of Photovoltaics* **8**, 1313.
[12] Prokscha T Morenzoni E, Deiters K, Foroughi F, George D, Kobler R, Suter A, Vrankovic V 2008, The new beam at PSI: a hybrid-type large acceptance channel for the generation of a high intensity surface-muon beam, *Nucl. Instrum. Methods Phys. Res. A* **595**, 317.
[13] Simões A F A, Alberto H V, Vilão R C, Gil J M, Cunha J M V, Curado M A, P.Salomé P M P, Prokscha T, Suter A, and Salman Z, 2020, Muon implantation experiments in films: obtaining depth-resolved information, *Rev. Sci. Instrum.* **91**, 023906.
[14] Martins, M I M 2020, Innovative dielectric materials for passivation of interfaces in solar cells: a μSR study, Master Thesis, University of Coimbra, Portugal, http://hdl.handle.net/10316/92546
[15] Ribeiro E, Alberto H V, Vilão R C, Gil J M, Weidinger A, Salomé P M P, Prokscha T, Suter A, and Salman Z, 2020, CdS versus ZnSnO buffer layers for a CIGS solar cell: a depth-resolved analysis using the muon probe, *EPJ Web of Conferences* **233**, 05004.
[16] Eckstein W, 1991 *Computer Simulations of Ion-Solid Interactions* (Springer, Berlin, Heidelberg, New York)
[17] Morenzoni E, Glückler E H, Prokscha T, Khasanov R, Luetkens H, Birke M, Forgan E M, Niedermayer Ch, Pleines M 2002, Implantation studies of keV positive muons in thin metallic layers, *Nucl. Instrum. Methods Phys. Res. B: Beam Interactions with Materials and Atoms* **192**, 254.
[18] Ribeiro E F M, Alberto H V, Vilão R C, Gil J M and Weidinger A 2022, Unfolding slow muon depth profiles with universal range distributions, to be submitted to *J. Phys.: Conf. Series* for the Conference Proceedings of the 15th International Conference on Muon Spin Rotation, Relaxation and Resonance, Parma, Italy.
[19] Vilão R C, Vieira R B L, Alberto H V, J. M. Gil J M , and Weidinger A, 2017, Role of the transition state in muon implantation, Phys. Rev. B **96**, 195205
[20] Vilão R C, Alberto H V, J. M. Gil J M , and Weidinger A, 2019, Thermal spike in muon implantation, Phys. Rev. B **99**, 195206.
[21] Vilão R C,Marinopoulos A G, Alberto H V, Gil J M, Lord J S and Weidinger A, 2021, Sapphire α-Al_2O_3 puzzle: Joint μSR and density functional theory study, Phys. Rev. B **103** 125202
[22] Marinopoulos A G, Vilão R C, Alberto H V, Ribeiro E F M, Gil J M, Mengyan P W, Goeks M R, Kauk-Kuusik M and Lord J S 2021, Hydrogen states in mixed-cation $CuIn_{(1-x)}Ga_xSe_2$ chalcopyrite alloys: a combined study by first-principles density-functional calculations and muon spectroscopy, *Philosophical Magazine* **101**, 2412.